



ESA Climate Change Initiative

Antarctica_Ice_Sheet_cci+ (AIS_cci+)

Science Highlights Phase 2 Year 1 (SH)

Prime & Science Lead: Andrew Shepherd
Northumbria University, Newcastle upon Tyne, United Kingdom

Technical Officer: Anna Maria Trofaier
ESA ECSAT, Didcot, United Kingdom

Consortium:
DTU Microwaves and Remote Sensing Group (DTU-N)
DTU Geodynamics Group (DTU-S)
Environmental Earth Observation IT GmbH (ENVEO)
Deutsches Zentrum für Luft- und Raumfahrt (DLR) Remote Sensing Technology
Institute (IMF)
Northumbria University (NU)
Science [&] Technology AS (ST)
Technische Universität Dresden (TUDr)
University College London (UCL/MSSL)



Signatures page

Prepared by	Andrew Shepherd Science Leader, NU	
Issued by	Daniele Fantin, Project Manager, S&T	
Approved by	Anna Maria Trofaier ESA Technical Officer	



Table of Contents

Change Log	4
Acronyms and Abbreviations	5
1 Introduction	7
1.1 Purpose and Scope	7
1.2 Document Structure	7
1.3 Applicable and Reference Documents	7
2 Scientific Highlights	8
2.1 SEC	8
2.2 IV and IVC	8
2.3 GMB	10
2.4 GLL	10
2.5 ISCL	11
3 CCI data links	13
4 References	14



Change Log

Issue	Author	Affected Section	Change	Status
0.6	S&T	All	Draft version	
1.0	All	All	First version	Released to ESA



Acronyms and Abbreviations

Acronym	Explanation
AIS	Antarctic Ice Sheet
ADP	Algorithm Development Plan
AIS_cci+	Antarctic Ice Sheets CCI project Extension
API	Antarctic Peninsula
ATBD	Algorithm Theoretical Basis Document
CAR	Climate Assessment Report
CCI(+)	Climate Change Initiative (Extension)
CFL	Calving Front Location
CONAE	Comisión Nacional de Actividades Espaciales
DEM	Digital Elevation Model
DLR	Deutsches Zentrum für Luft- und Raumfahrt
DTU	Danish Technical University
EAIS	East Antarctic Ice Sheet
ECV	Essential Climate Variable
ENVEO	ENVironmental Earth Observation GmbH
EO	Earth Observation
ESA	European Space Agency
GLL	Grounding Line Location
GLM	Grounding Line Migration
GMB	Gravimetric Mass Balance
ISCL	Ice Shelf Coast Line
IV	Ice Velocity
IV-TDM	Ice Velocity Tidal Correction Module
IVC	Ice Velocity Change
MFID	Mass Flux Ice Discharge
MPC	Mission Performance Cluster
SEC	Surface Elevation Change
SL	Science Lead
SOW	Statement of Work
ST	Science & Technology AS
TOPS	Terrain Observation by Progressive Scans
TUD	Technical University of Dresden
UB	University of Bristol
UCL	University College London
UL	University of Leeds
UN	University of Northumbria
WAIS	West Antarctic Ice Sheet
NASA	National Aeronautics and Space Administration



SAR	Synthetic Aperture Radar
InSAR	Interferometric SAR
ML	Machine Learning



1 Introduction

1.1 Purpose and Scope

This document represents a description of Science Highlights (SH) for year 1 activities of the Antarctica_Ice_Sheet_cci (AIS_cci) project for CCI+ Phase 2, in accordance to contract and SoW [AD1 and AD2]. The central aim is to provide science highlights designed for public consumption, including illustrating images and appropriate links for more details.

1.2 Document Structure

This document is structured into a single chapter describing the following scientific highlight from:

- Surface Elevation Change (SEC)
- Ice Velocity (IV)
- Ice Velocity Change (IVC)
- Gravimetric Mass Balance (GMB)
- Grounding Line Location (GLL)
- Ice Shelf CoastLines (ISCL)

1.3 Applicable and Reference Documents

Table 1.1: List of Applicable Documents

No	Doc. Id	Doc. Title	Date	Issue/ Revision/ Version
AD1	ESA/Contract No. 4000143397/23/I-NB CCI+ PHASE 2 - AIS	CCI+ PHASE 2 - NEW R&D ON CCI ECVS for AIS CCI	13.02.2024	NA
AD2	ESA-EOP-SC-AMT-2023-12 and its appendix 2	STATEMENT OF WORK, ESA EXPRESS PROCUREMENT – EXPRO CCI+ Phase 2 – Theme II – Antarctic Ice Sheet (AIS)	14.07.2023	1.2

Note: If not provided, the reference applies to the latest released Issue/Revision/Version



2 Scientific Highlights

This report summarizes scientific papers per ECV.

2.1 SEC

Although fluctuations in ice sheet surface mass balance lead to seasonal and interannual elevation changes, it is unclear if they are resolved differently by radar and laser satellite altimeters. **Ravinder *et al.*** compare methods of computing elevation change from CryoSat-2 and ICESat-2 over the Greenland Ice Sheet to assess their consistency and to quantify recent change. Solutions exist such that interannual trends in the interior and the ablation zone agree to within -0.2 ± 1.5 and 3.3 ± 6.0 cm/yr, respectively, and that seasonal cycle amplitudes within the ablation zone agree to within 3.5 ± 38.0 cm. The agreement is best in the north where the measurements are relatively dense and worst in the southeast where the terrain is rugged. Combining data from both missions, the authors estimate Greenland lost 196 ± 37 km³/yr of volume between 2010 and 2022 with an interannual variability of 129 km³/yr.

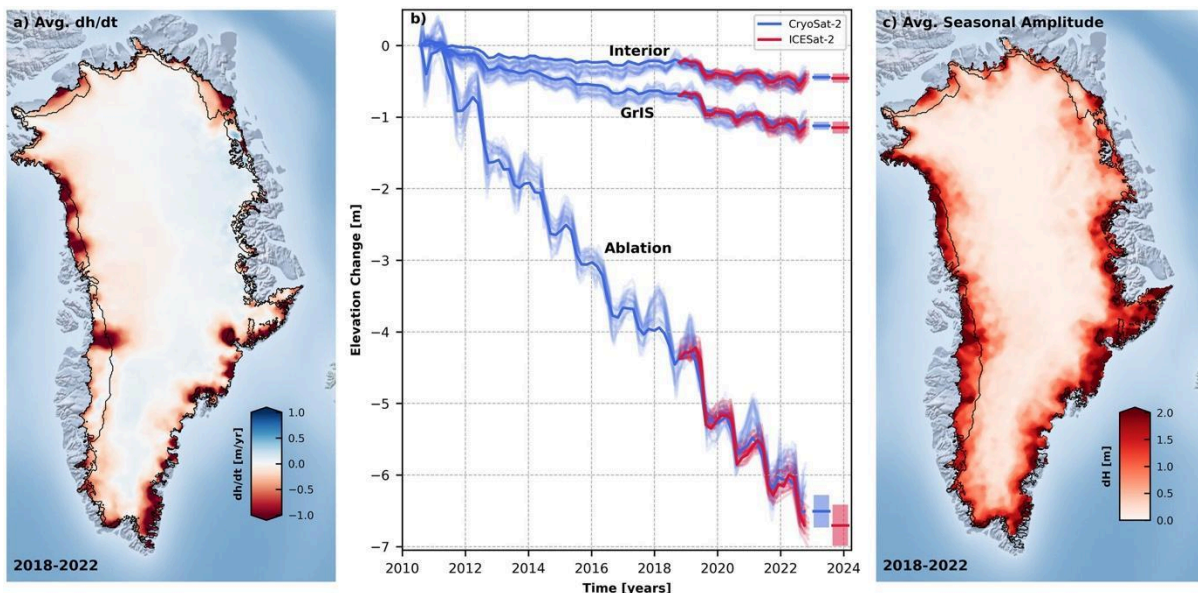


Figure 2.1 Rates of elevation change averaged from CryoSat-2 and ICESat-2 between 2018 and 2022 (a). Time series of bi-monthly elevation changes (b) from CryoSat-2 (blue) and ICESat-2 (red); the preferred scenarios are shown in dark lines with the shaded bands showing the respective uncertainties, and the ensemble scenarios are in shaded lines. Amplitudes of seasonal cycle averaged from both missions (c). A 25×25 km median filter is applied to both (a) and (c) for visualization.

2.2 IV and IVC

The January 2022 disintegration of multi-year landfast sea ice in the Larsen B embayment, Antarctic Peninsula, was closely followed by a significant acceleration of ice flow and ice-front retreat of numerous outlet glaciers. Crane Glacier was a notable example of this, with 6 km of its floating ice shelf lost to calving in the first month following the disintegration and a 3.4 % increase in terminus flow speeds over the same time period. **Parsons *et al.***, for the first time, quantify the buttressing stresses that were transmitted to Crane by the ice melange at the glacier outlet using the ice-flow model Úa. The model is constrained with

high-resolution surface elevation profiles of the glacier and ambient melange, while the observed flow velocities are reconstructed by optimising the rheology rate factor throughout the model domain thus allowing the authors to quantify the stress regime across both the glacier and ice melange. Results showed that resistive backstresses were imparted to Crane by the ice melange with a mean buttressing ratio of $\Theta_N=0.68$ calculated at the glacier terminus ($\Theta_N=1$ implies no buttressing). In addition, diagnostic modelling showed an expected 19.2 kPa mean increase in extensional stress at the ice front following the disintegration of the ice melange. This perturbation in stress likely triggered the observed rapid calving over the near-terminus region, leading to the periodic loss of sections of Crane's buttressing ice shelf and thus further acceleration of ice flow in the subsequent months.

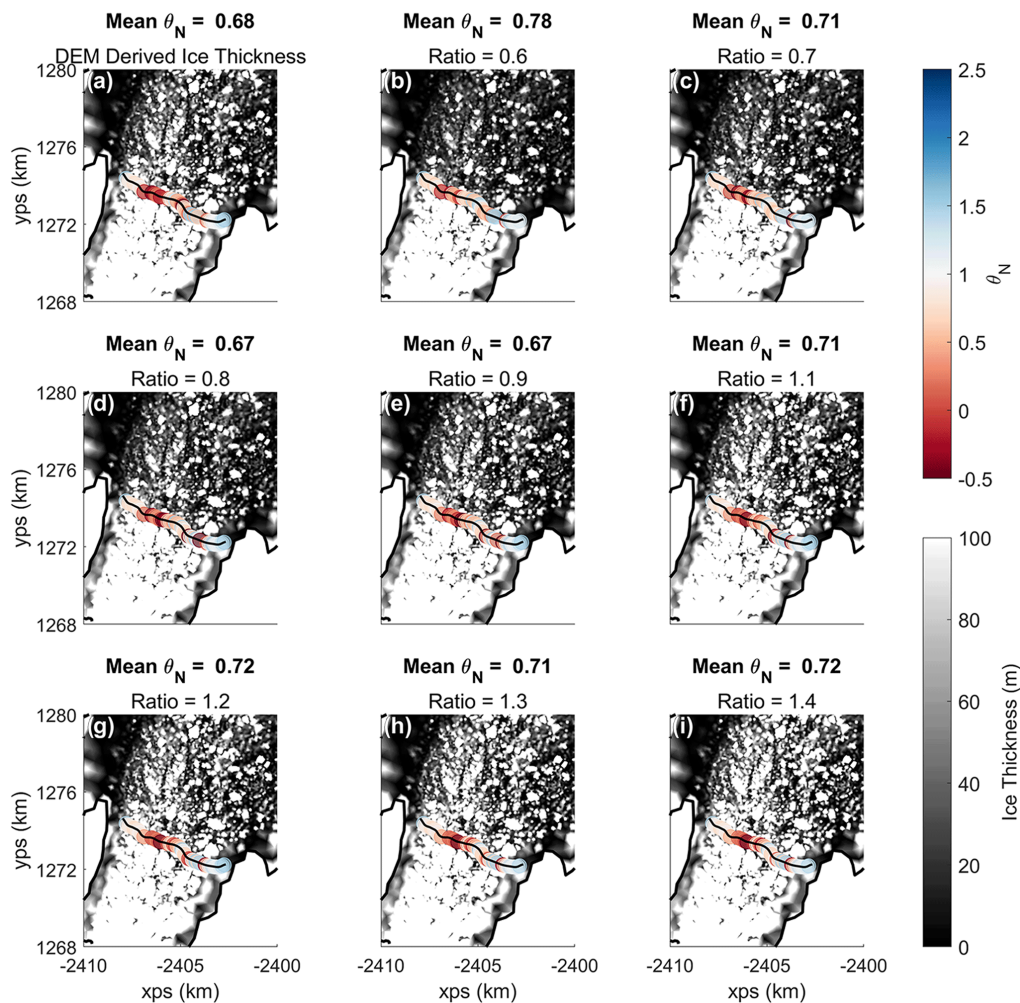


Figure 2.2. The buttressing numbers calculated at the December 2021 terminus location with sea ice represented by varying ice thicknesses in the model. Updated model inversions were performed separately for each configuration. In panel a), the sea ice and melange thicknesses downstream of the terminus were defined using the REMA strip DEMs as per the initial intact model configuration. In panels b) - i) Ice thicknesses downstream of the terminus were adjusted from the DEM derived thickness by the ratio displayed on each panel. The dashed yellow line shows the terminus location with buttressing numbers along this line shown by coloured bubbles at 100 m intervals.



2.3 GMB

A detailed understanding of how the Antarctic ice sheet (AIS) responds to a warming climate is needed because it will most likely increase the rate of global mean sea level rise. Time-variable satellite gravimetry, realized by the Gravity Recovery and Climate Experiment (GRACE) and Gravity Recovery and Climate Experiment Follow-On (GRACE-FO) missions, is directly sensitive to AIS mass changes. However, gravimetric mass balances are subject to two major limitations. First, the usual correction of the glacial isostatic adjustment (GIA) effect by modelling results is a dominant source of uncertainty. Second, satellite gravimetry allows for a resolution of a few hundred kilometres only, which is insufficient to thoroughly explore the causes of AIS imbalance.

Willem *et al.* overcome both limitations by the first global inversion of data from GRACE and GRACE-FO, satellite altimetry (CryoSat-2), regional climate modelling (RACMO2), and firn densification modelling (IMAU-FDM). The inversion spatially resolves GIA in Antarctica independently from GIA modelling jointly with changes of ice mass and firn air content at 50 km resolution. The authors find an AIS mass balance of $-144 \pm 27 \text{ Gt a}^{-1}$ from January 2011 to December 2020. This estimate is the same, within uncertainties, as the statistical analysis of 23 different mass balances evaluated in the Ice sheet Mass Balance Inter-comparison Exercise (IMBIE; [Otosaka *et al.*, 2023b](#)). The co-estimated GIA corresponds to an integrated mass effect of $86 \pm 21 \text{ Gt a}^{-1}$ over Antarctica, and it fits better with global navigation satellite system (GNSS) results than other GIA predictions. From propagating covariances to integrals, **Willem *et al.*** find a correlation coefficient of -0.97 between the AIS mass balance and the GIA estimate. Sensitivity tests with alternative input data sets lead to results within assessed uncertainties.

2.4 GLL

Antarctica has an active subglacial hydrological system, with interconnected subglacial lakes fed by subglacial meltwater. Subglacial hydrology can influence basal sliding, inject freshwater into the sub-ice-shelf cavity, and impact sediment transport and deposition which can affect the stability of grounding lines (GLs). **Freer *et al.*** use satellite altimetry data from the ICESat, ICESat-2, and CryoSat-2 missions to document the second recorded drainage of Engelhardt Subglacial Lake (SLE), which began in July 2021 and discharged more than 2.3 km^3 of subglacial water into the Ross Ice Shelf cavity. The authors used different synthetic aperture radar interferometry from RADARSAT-2 and TerraSAR-X alongside ICESat-2 repeat-track laser altimetry (RTLA) and REMA digital elevation model strips to detect 2–13 km of GL retreat since the previous drainage event in 2003–06. Combining these satellite observations, the mechanism triggering SLE drainage, the cause of the observed GL retreat, and the interplay between subglacial hydrology and GL dynamics is evaluated. The authors find that: (a) SLE drainage was initiated by influx from a newly identified upstream lake; (b) the observed GL retreat is mainly driven by the continued retreat of Engelhardt Ice Ridge and long-term dynamic thinning that caused a grounded ice plain to reach flotation; and (c) SLE drainage and GL retreat were largely independent. **Freer *et al.*** also discuss the possible origins and influence of a 27 km grounded promontory found to protrude seaward from the GL.

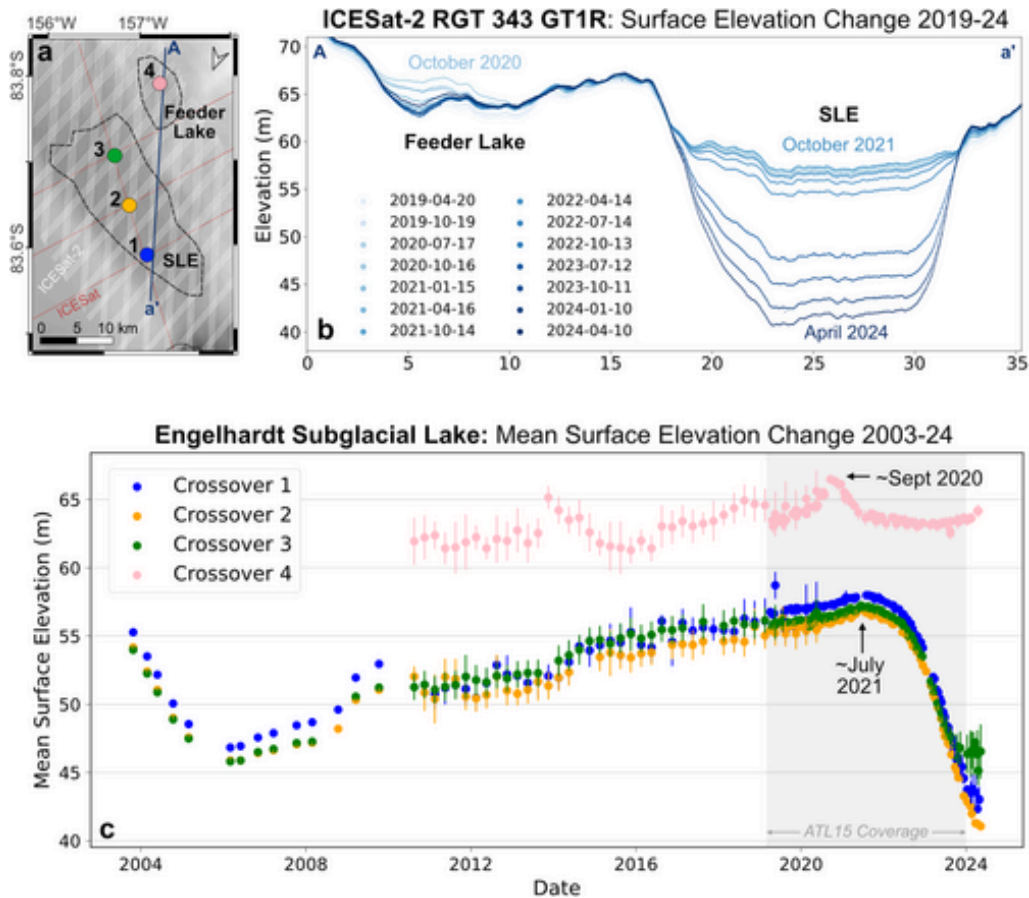


Figure 2.3. Satellite laser and radar altimetry measurements of surface elevation change at SLE, 2003–24. (a) Location of the four crossover zones (CZ1–4) used to calculate mean elevation change at SLE, and ICESat (red) and ICESat-2 (white) RGTs. (b) Repeat surface elevation profiles along ICESat-2 RGT 343 ground track 1R (GT1R), April 2019–April 2024; location in (a). (c) 21-year time-series of mean surface elevation at SLE, measured within CZ1–4 by ICESat (2003–09), CryoSat-2 (2010–20) and ICESat-2 (2019–24). Error bars represent one standard deviation of along-track surface elevation measurements within each CZ (note error bars are too small to be visible for some ICESat and ICESat-2 data points). Grey shading shows the ICESat-2 ATL15 coverage period.

2.5 ISCL

Research on delineating ice shelf calving lines focuses on using Synthetic Aperture Radio (SAR) imagery from the Sentinel-1 satellite as well as ice elevation data from the CryoSat-2 satellite to feed an iterative refinement-based U-Net CNN that predicts the location of these calving fronts. The area of interest includes 3 ice shelves (Ronne, LarsenC, and Filchner). The data from Sentinel-1 was already collected, preprocessed, and filtered. The Track elevation data from CryoSat2 was also collected, preprocessed, and interpolated across time to create 2D elevation maps for the concerned areas at each time (in the ice shelf areas typical DEMs won't do since ice shelves drift and change frequently). Label data were also collected and processed (the IceLines daily data). The network was created and preliminary results were acquired by combining both data sources. Figure 2.4 shows the IceLines delineation (coloured lines) on top of a SAR image (black and white) of the Filchner ice shelf. It can be seen that some of these lines are inaccurate and have problematic results. Although we have this data as labels, we hope to improve upon it with various pseudo-labelling techniques. Figure 2.5 shows the iterative refinement method adopted by our model to fit the preliminary prediction from the elevation data (CryoSat2) into the Ice shelf coastline with the Sentinel-1 SAR data.

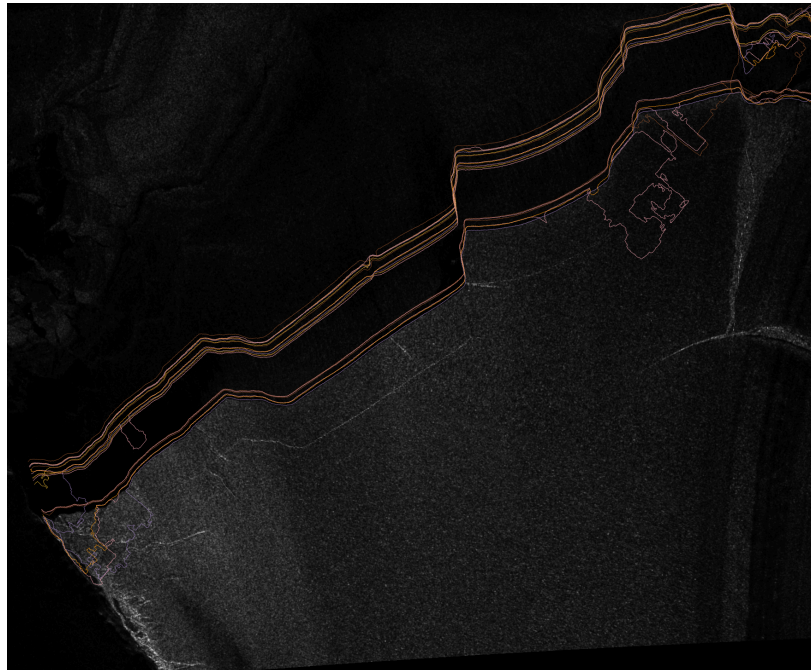


Figure 2.4: Filchner Ice Shelf with delineations of its calving front for various days.



Figure 2.5: Iterative refinement fitting the ISCL to its correct location.



3 CCI data links

This section provides access to various datasets published by the Antarctic Ice Sheet ECV project.

Samples of the project's datasets are also available on the [ESA Climate Office Open Data Portal](#).

- SEC products are hosted by [CPOM](#).
- IV products are provided on ENVEO [CryoPortal](#) and [CEDA](#).
- GMB products are hosted by [TU Dresden](#).



4 References

Freer, B. I. D., Marsh, O. J., Fricker, H. A., Hogg, A. E., Siegfried, M. R., Floricioiu, D., Sauthoff, W., Rigby, R., & Wilson, S.F. (2024). Coincident lake drainage and grounding line retreat at Engelhardt Subglacial Lake, West Antarctica. *Journal of Geophysical Research: Earth Surface*, **129**.

Ravinder, N., Shepherd, A., Otosaka, I., Slater, T., Muir, A., & Gilbert, L. (2024). Greenland Ice Sheet elevation change from CryoSat-2 and ICESat-2. *Geophysical Research Letters*, **51**.

Parsons, R., Sun, S., Gudmundsson, G. H., Wuite, J., & Nagler, T. (2024). Quantifying the buttressing contribution of sea ice to Crane Glacier, Antarctica Peninsula. *The Cryosphere*, **18**, 5789-5801.

Willen, M. O., Horwath, M., Buchta, E., Scheinert, M., Helm, V., Uebbing, B., & Kusche, J. (2024). Globally consistent estimates of high-resolution Antarctic ice mass balance and spatially-resolved glacial isostatic adjustment. *The Cryosphere*, **18**, 775-790.

Wuite, J., Nagler, T., Hetzenecker, M., & Rahim, T. (2024). Ice velocity, discharge & surface melt dynamics from EO data status & opportunities of upcoming sensors. European Polar Science Week Copenhagen Denmark 3-6 Sept 2024.



End of document